2nd Micro and Nano Flows Conference
West London, UK, 1-2 September 2009
Keynote Contribution

Local Heating Effects on Flow and Heat Transfer in Microchannels

X.F. PENG [1,*], J.T. LIU [1]

* Corresponding author: Tel/Fax: ++86 (10) 6278-9751; Email: pxf-dte@mail.tsinghua.edu.cn
1: Lab of Phasechange & Interfacial Transport Phenomena, Tsinghua University, Beijing 100084, China

Abstract A series of numerical investigations was conducted to explore the effects of temperature-dependent viscosity and thermal conductivity on two-dimensional low Reynolds number convection of water in microchannels with locally heating. An emphasis was addressed on the fundamental characteristics of flow and thermal re-development at different localized heat fluxes and different inlet temperatures. The velocity field is highly coupled with temperature distribution and distorted through the variations of viscosity and thermal conductivity. The induced cross-flow velocity has a marked contribution to the convection. The heat transfer enhancement due to viscosity-variation is pronounced, though the axial convection introduced by thermal-conductivity-variation is insignificant unless for the cases of very low Reynolds numbers. The heat transfer enhancement is described by defining the peak value and location of relative Nusselt number distribution as $\Delta Nu\%_{max}$ and X_{max}. Strong nonlinear interaction mechanism prevails in the correlation of $\Delta Nu\%_{max}$ and X_{max} due to high heat flux condition and dramatic rise of liquid temperature.

Keywords: Convection, Microchannel, Temperature-dependent property, Flow and thermal re-development, Entrance effect

1. Introduction

Since the pioneer work of Tuckerman and Pease (1981), and Wu and Little (1983, 1984), the application of microchannel heat sinks has been drawing increasing attention as one of the most promising high-efficiency heat exchange technologies, e.g., cooling of electronic devices, automotive heat exchangers, laser process equipments, and aerospace technology, etc.. In available literature there are many comprehensive investigations experimentally and theoretically performed by different researchers (Pfahler et al., 1990; Rahman and Gui 1993; Peng and Wang, 1993, 1994; Harms et al., 1997; Adams et al., 1998), and these are categorized into various topics focusing on some special aspects and elaborately summarized in the comprehensive review of Sobhan and Garimella (2001). Both friction behavior and heat transfer performance were the most concerned issues in these investigations, whose derivation from classical theory and the dependency on the channel diameter were not conclusive due to the different or even contradictory suggestions provided by different investigators (Palm, 2001).

Besides the reasonable suspecting on the quality of measured data, several possible explanations were provided for the derivations from classical theory, or so-called microscale effects. Some attributed the derivations to wall roughness, since the same absolute surface roughness has enlarged effect on small diameter channels than on large ones, as in the work of Kandlikar et al. (2003). Electric double-layer (EDL) effect was considered as an important factor or a body force term in the momentum equation to obtain the Nusselt number and friction factor for an aqueous solution of low ionic concentration and a wall surface of high zeta potential (Yang et al., 1998; Ng and Tan, 2004; Tan and Ng, 2006). However, it was also noted that for the conditions used in the evaluation of the model, EDL effects should not be important for pressure drop or heat transfer in channels larger than 40 μm.

Flow development of hydraulic and thermal boundary layers, or actually entrance effect is considered important in microchannel

convections, which are often characterized by laminar flow. Fedorov and Viskanta (2000) reported a substantial developing flow effect in the channels from their three-dimensional numerical simulations. Similar conclusion was drawn in the numerical investigation of Qu and Mudawar (2002). In their recent work (2006), collaborated with other authors, they conducted experimental and computational studies on flow development and pressure drop for adiabatic single-phase water flow in a single rectangular microchannel having 222μm wide, 694μm deep, and 12 cm long at Reynolds numbers ranging from 196 to 2215. The velocity field was measured using a micro-particle image velocimetry system. Pronounced evidence was provided to demonstrate the strong entrance effect from their experiments and numerical simulations. Gamrat et al. (2005) performed both two- and three- dimensional numerical analysis of microchannel convection, considering the thermal entrance effects and conjugate heat transfer of fluid and solid wall. Their results, together with those above-mentioned, confirm that the continuum model of conventional mass, Navier-Stokes and energy equations are of adequate accuracy in representing the microchannel flow and heat transfer characteristics.

The practical operation of microchannel devices, especially for liquids as working fluids, is generally characterized with low Reynolds number flow and high heat flux. One consequence of such conditions is the large variation of liquid properties, at least the viscosity and thermal conductivity, due to steep temperature gradient. Then constant thermophysical properties, usually used in the most available analyses, could not fully reveal the characteristics of fluid flow and heat transfer in the conditions of high heat flux and low Reynolds number flow, implying large variation of liquid properties. As a result, the momentum equation is no longer independent of the energy equation in the conservative model, drawing significant difficulty in the theoretical analysis. For water in the temperature range from 0 to 100 ℃, μ varies by 84%(decrease), k by 21%(increase), ρ by 4%(decrease) and c_p by 1%(non-monotonic) (Wagner and Berlin, 1998). The relatively large variations of μ and k should be treated as functions of temperature.

Traditionally, the property-ratio method and reference temperature method (Sieder and Tate, 1936; Shah and London, 1978) used to be employed to the correction of Nusselt number for convection in conventional tubes. Herwig (1985) proposed an Asymptotic Theory method. Due to the empirical nature of these methods and/or failure to provide reasonable prediction for large heat flux, Mahulikar and Herwig (2005) established a continuum-based model for laminar convections, incorporating temperature dependence of fluid viscosity and thermal conductivity. The solution of the model relied on mature computational fluid dynamics technology and showed applicability for a large range of heat flux, indicating its suitable usage in microchannel convections. In their most recent work (Mahulikar and Herwig, 2006; Herwig and Mahulikar, 2006), detailed effects of temperature-dependent properties were provided on the fully developed laminar micro-convection in circular tubes.

Non-uniform heating conditions are another important feature in the practical operation of microchannel devices in terms of both space and time scales. However, uniform thermal boundary was usually assumed in the available investigations, either isothermal or uniform heat flux condition. The non-uniformity of thermal boundary conditions would remarkably alter the temperature distribution of the fluid, and additionally alter the flow field through the variation of μ and k.

More robust treatment on the variable-property flow and heat transfer problems was implemented by the mature development of modern computation technology, e.g., the Computational Fluid Dynamics and Numerical Heat Transfer methods. In the last decade, the effects of temperature-dependent fluid properties were emphasized in many micro- and pore-scale numerical researches. Nonino et al. (2006) performed an investigation on the effects of temperature dependent viscosity in simultaneously developing liquid laminar flow

in straight ducts, and noted that the effects of temperature dependent viscosity were non-negligible on laminar forced convection within a wide range of operative conditions. They further investigated viscous dissipation in a similar application (Del Giudice et al., 2007). Kumar et al. (2007) studied the heat transfer and fluid flow with temperature-dependent properties in helical coil tubes at low-Reynolds numbers. The variation in thermophysical properties of water and diethylene glycol induces marked impact on the friction factor and Nusselt number, as well as the secondary flow profile. For steady laminar-boundary-layer flow over a moving isothermal flat plat in the presence of a magnetic field, Seddeek and Salem (2006) found that the variable viscosity effect has to be taken into consideration. Pantokratoras (2007) numerically investigated the steady laminar flow in a fluid-saturated porous medium channel between two parallel plates, concerning engine oil, water and air, with the variation of their physical properties with temperature. It was found that the temperature-dependent viscosity and, in some cases, density and thermal conductivity played important roles when the temperature difference between the plates was large.

Based on a similar theoretical model, Liu et al. (2007, 2008) conducted numerical investigation on variable-property laminar convection study in 2-D microchannels under Cartesian coordinates. They presented the single-hump-shaped distribution of local relative Nusselt number enhancement due to property variation, and further clarified the role of inlet Reynolds number. The axial conduction due to thermal-conductivity variation showed relatively low significance, simply because the Peclet number was larger than 50 within the operation range of their study.

In the present work a series of numerical investigations was conducted for the two-dimensional low Reynolds number convection of water in microchannel with the combination of locally heated wall boundary condition and temperature-dependent viscosity and thermal conductivity. Heat transfer performance was evaluated by comparing with constant-property solutions. The effect of thermal development and property variation was discussed through detail analysis of local momentum and heat transport.

2. Fundamental Considerations

2.1 Fundamental considerations

Thermally developing and hydrodynamic-cally developed flow is commonly encountered in practical microchannel heat sinks and other associated applications, due to non-uniform heating conditions in terms of space and time scales. The problem is also termed as thermal entrance problem, or Graetz-type problem, following the first work by Graetz (1883) in 1883 and Nusselt (1910) in 1910. Only energy equation is solved in the classical treatment of this kind of problem, by assuming unchanged parabolic velocity profile along the flow. However, in the variable-property thermal entrance problem, as investigated in present work, the flow and energy equations are fully coupled with each other through the temperature-dependent viscosity. Therefore, both hydrodynamic and thermal boundary development take place along the heated channel, regardless of fully-developed inlet velocity condition. For the convenience of discussion, a two-dimensional model was set up on a two-parallel-plate domain, with equations and boundary conditions specified in the following sections.

2.2 Equations and boundary conditions

The model was derived from continuum-based conservation equations of mass, momentum and energy (Sherman, 1990), with the following basic assumptions:

1) Incompressible Newtonian fluid and steady laminar flow;
2) Constant specific heat of the fluid;
3) Thermal conductivity and viscosity are the single variable functions of temperature;
4) Negligible effect of gravity and other forms of body forces.

The resulting governing equations are:

Continuity equation

$$\nabla \cdot \mathbf{u} = div\mathbf{u} = 0 \quad (1)$$

Momentum equation

$$\rho(\mathbf{u}\cdot\nabla)\mathbf{u} = -\nabla p + \mu\nabla^2\mathbf{u} + S_\mu \nabla T \cdot \mathrm{def}\,\mathbf{u} \quad (2)$$

Energy equation

$$\rho c_p (\mathbf{u}\cdot\nabla)T = k\nabla^2 T + S_k \nabla T\cdot\nabla T + \Phi \quad (3)$$

where, S_μ=dμ/dT, is viscosity-temperature sensitivity; S_κ=dk/dT, thermal-conductivity-temperature sensitivity; $\Phi = \mu \mathrm{def}\,\mathbf{u} : \mathrm{def}\,\mathbf{u}/2$, viscous dissipation term; $\mathrm{def}\,\mathbf{u} = \nabla\mathbf{u} + (\nabla\mathbf{u})^T$, rate of deformation tensor.

By restricting the discussion within two-dimensional space, and applying the following dimensionless groups,

$$\mathbf{R} = X\mathbf{e}_i + Z\mathbf{e}_k = \mathbf{r}/D = x/D\mathbf{e}_i + z/D\mathbf{e}_k$$
$$\mathbf{U} = U\mathbf{e}_i + W\mathbf{e}_k = \mathbf{u}/u_0 = u/u_0\mathbf{e}_i + w/u_0\mathbf{e}_k,$$
$$\theta = \frac{k_0(T-T_0)}{q_w'' D},\quad k^* = k/k_0,\quad \mu^* = \mu/\mu_0,$$
$$P = p/p_a, S_\mu^* = S_\mu/S_{\mu,0},\quad S_k^* = S_k/S_{k,0} \quad (4)$$

the governing equations are then non-dimensionalized as the follows:

Continuity equation

$$\frac{\partial U}{\partial X} + \frac{\partial W}{\partial Z} = 0 \quad (5)$$

X-component momentum equation

$$U\frac{\partial U}{\partial X} + W\frac{\partial U}{\partial Z} = -\mathrm{Eu}\frac{\partial P}{\partial X} + \frac{\mu^*}{\mathrm{Re}_D}\left(\frac{\partial^2 U}{\partial X^2} + \frac{\partial^2 U}{\partial Z^2}\right) + \frac{1}{\mathrm{Re}_D}\frac{\mathrm{Br}_{S\mu}}{\mathrm{Br}_{qw}} S_\mu^*\left[2\frac{\partial\theta}{\partial X}\frac{\partial U}{\partial X} + \frac{\partial\theta}{\partial Z}\left(\frac{\partial U}{\partial Z} + \frac{\partial W}{\partial X}\right)\right] \quad (6)$$

Z-component momentum equation

$$U\frac{\partial W}{\partial X} + W\frac{\partial W}{\partial Z} = -\mathrm{Eu}\frac{\partial P}{\partial Z} + \frac{\mu^*}{\mathrm{Re}_D}\left(\frac{\partial^2 W}{\partial X^2} + \frac{\partial^2 W}{\partial Z^2}\right) + \frac{1}{\mathrm{Re}_D}\frac{\mathrm{Br}_{S\mu}}{\mathrm{Br}_{qw}} S_\mu^*\left[\frac{\partial\theta}{\partial X}\left(\frac{\partial W}{\partial X} + \frac{\partial U}{\partial Z}\right) + 2\frac{\partial\theta}{\partial Z}\frac{\partial W}{\partial Z}\right] \quad (7)$$

Energy equation

$$U\frac{\partial\theta}{\partial X} + W\frac{\partial\theta}{\partial Z} = \frac{k^*}{\mathrm{Re}_D\,\mathrm{Pr}}\left(\frac{\partial^2\theta}{\partial X^2} + \frac{\partial^2\theta}{\partial Z^2}\right) + \frac{1}{\mathrm{Re}_D\,\mathrm{Pr}}\left\{\frac{\mathrm{Br}_{Sk}}{\mathrm{Br}_{qw}} S_k^*\left[\left(\frac{\partial\theta}{\partial X}\right)^2 + \left(\frac{\partial\theta}{\partial Z}\right)^2\right] + \Phi^*\right\} \quad (8)$$

Where the Φ stands for the viscous dissipation term,

$$\Phi^* = \mathrm{Br}_{qw}\mu^*\left[2\left(\frac{\partial U}{\partial X}\right)^2 + 2\left(\frac{\partial W}{\partial Z}\right)^2 + \left(\frac{\partial W}{\partial X} + \frac{\partial U}{\partial Z}\right)^2\right] \quad (9)$$

and the dimensionless governing parameters are defined as,

$$\mathrm{Br}_{qw} = \frac{u_0^2\mu_0}{q_w'' D},\quad \mathrm{Br}_{S\mu} = \frac{S_{\mu,0}u_0^2}{k_0},\quad \mathrm{Br}_{Sk} = \frac{S_{k,0}\mu_0 u_0^2}{k_0^2},$$
$$\mathrm{Re}_D = \frac{\rho u_0 D}{\mu_0},\quad \mathrm{Pr} = \frac{c_p\mu_0}{k_0},\quad \mathrm{Eu} = \frac{p_a}{\rho u_0^2} \quad (10)$$

The Br_{qw} is the Brinkman number based on wall heat flux, and $Br_{S\mu}$ and Br_{Sk} are modified Brinkman numbers based on viscosity-temperature and conductivity-temperature sensitivity, respectively. In the dimensionless form of conservative equations, Br_{qw} appears as a multiplier to the viscosity dissipation term, while its reciprocal appears before the temperature terms that indicate the significance of variation in fluid properties. When Br_{qw} is about or even larger than unity, the momentum transfer across flow is comparable to heat transfer from the wall, and the momentum transfer results in significant viscous dissipation (Bird et al., 2002). When Br_{qw}<<1, the coupling effect of energy transport on momentum transport increases through the variation of μ. Thus for a typical application of microchannels, high heat flux and low flow velocity always result in a small value of Br_{qw}, which indicates strong influence of property variation on the convection. $Br_{S\mu}$ and Br_{Sk} show the relative importance of momentum transport across the flow due to viscosity and thermal-conductivity variation, over the energy transport due to the fluid conduction, respectively. Elaborated physical significance of the Brinkman numbers could be found in Mahulikar and Herwig (2005).

Water was used as working liquid in this simulation. The viscosity and thermal conductivity were calculated by the IAPWS-IF97 method (Wagner and Berlin, 1998) in the temperature range of liquid water, i.e., from 0 to 100 ℃.

The governing equations were solved in the domain shown in Fig. 1. Taking the advantage of symmetry, only half of the channel is modeled. The channel wall was divided into three sections. The center region was heated at constant heat flux, q''_w, while the upstream and downstream regions were adiabatic walls. The length of the heated region was fixed at 20*D*. The lengths of the upstream and downstream region are both set as 10*D*, which were selected based on a compromise between computation cost and the requirement for numerical stability. No slip condition was set for all the three sections. The origin of the two-dimensional rectangular coordinate system was located at the start point of the heated region on the centerline (symmetric plane), with the *x*-axis running along the channel.

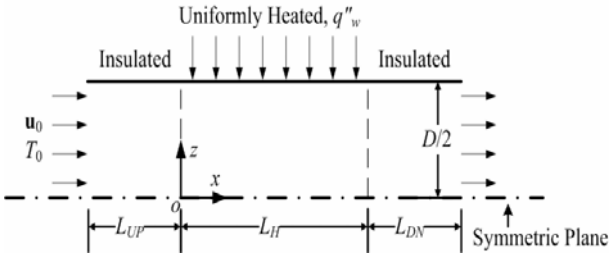

Fig. 1. Physical model

At the entrance (*X*=-10) of the channel, the fully-developed flow condition was assumed with uniform temperature, given as,

$$U = 1.5(1-4Z^2) \quad (11a)$$

$$W = 0 \quad (11b)$$

$$\theta = 0 \quad (11c)$$

At the exit (*X*=30), the axial gradients for all the transport variables except pressure were assumed to be zero.

2.3 Properties

The temperature dependency of viscosity for liquid water is given as (Sherman, 1990),

$$\mu(T) = \mu(T_{\text{ref}})\left(\frac{T}{T_{\text{ref}}}\right)^n \exp\left[B\left(T^{-1} - T_{\text{ref}}^{-1}\right)\right] \quad (12)$$

where n=8.9, B=4700 K, $\mu(T_{\text{ref}})=1.005\times10^{-3}$ kg/ms, T_{ref}=293 K. The temperature-dependent thermal conductivity is given by a cubic polynomial fitting result of data (Holman, 1997) in the following form,

$$k(T) = a_0 + a_1 T + a_2 T^2 + a_3 T^3 \quad (13)$$

where $a_0 = -1.135$, $a_1 = 0.01154$, $a_2 = -2.375\times10^{-5}$ and $a_3 = 1.571\times10^{-8}$.

2.4 Performance parameters

The influence of the μ- and k-variations on the local heat transfer in a microchannel is the focused issue in this investigation. Apparently, the local Nusselt number is an important parameter and defined as,

$$\text{Nu} = \frac{hD}{k_m} = \frac{q''_w D}{k_m\left(T_w - T_b\right)} = \frac{1}{k_m^*\left(\theta_w - \theta_b\right)} \quad (14)$$

where non-dimensionless wall and bulk temperatures are defined as the follows,

$$\theta_w = \frac{k_0\left(T_w - T_0\right)}{q''_w D}, \theta_b = \frac{k_0\left(T_b - T_0\right)}{q''_w D} = \int_0^1 U\theta dZ \quad (15)$$

And the relative difference of local *Nu* for variable-property and constant-property is defined as the follows,

$$\Delta\text{Nu}\% = \frac{\text{Nu} - \text{Nu}_{\text{CP}}}{\text{Nu}_{\text{CP}}}\times100\% \quad (16)$$

Eq. (16) is used to more clearly and quantitatively describe the effect of variable fluid properties on the heat transfer characteristics.

2.5 Numerical method and validation

The governing equations with boundary conditions were solved by the commercial CFD code, CFX5. The governing equations were discretized by means of a fully implicit second order finite volume method with modified upwind advection scheme. The grid points used in the *x* and *z* directions were selected to be 600 and 70, respectively, with carefully distributed density near the central heated region. The effects of the grid numbers on the simulation accuracy were examined and the maximum deviations of the predicted local Nusselt number were less than 0.014% among the computations on the grids of 240×50, 600×50, 600×70, 600×100 and 900×70. Therefore, the grid system of 600×70 points seemed to be sufficient to resolve the behavior of the fluid flow and heat transfer in

microchannels. A converged solution was obtained using this grid, with root mean square residuals less than 10^{-7} for all the transport variables and independent of the iteration numbers, and domain imbalances of mass, momentum and energy conservation less than 10^{-7}.

The validation of the numerical method was performed using water with constant properties and uniform heat flux condition over the entire channel wall, as a benchmark case. The temperature profile in the fully-developed region of the channel showed excellent agreement with analytical solution. The Nusselt number obtained from simulation agreed with the theoretical value, $Nu_{CP,FD}$=70/17 (Arpaci and Larsen, 1984) with an relative error lower than 0.05%.

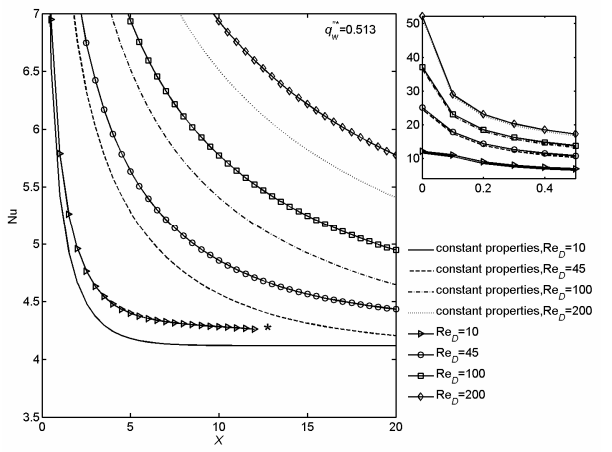

(a) Local *Nu*

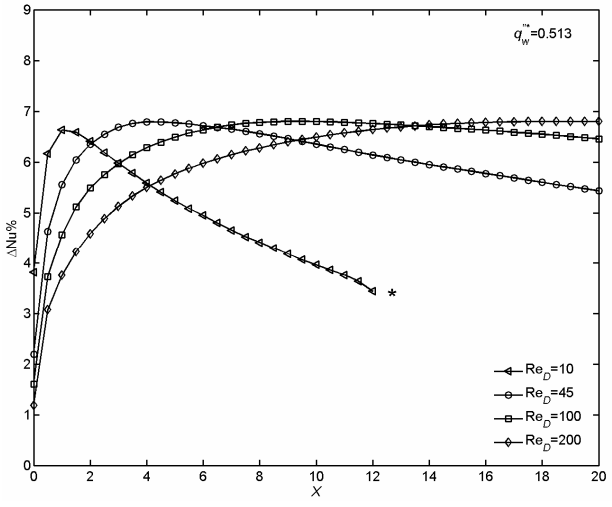

(b) Local Δ*Nu*% with *X*

Fig. 2. Effect of property on heat transfer

Apparently, the solution method and the formulae adopted were appropriate for the present study. For all investigated cases, the channel width, D was 100 μm, and inlet velocity u_0=0.455 m/s. Inlet temperature and heat flux varied within the range of 20 to 70 ℃ and 3 to 9×10^5 W/m^2, respectively.

3. Heat Transfer Enhancement

For all tested cases in this work, the channel width, D, was 100μm, and inlet temperature, T_0=20 ℃. The Reynolds number, Re_D and heat flux were altered to examine the effects of property variation within the temperature range of liquid water. For the convenience of comparison with other researches, the heat flux was non-dimensionalized as the following form,

$$q_w''^* = \frac{q_w'' D}{k_0 T_0} \tag{17}$$

which ranged from 0.057 to 0.855.

3.1 Heat transfer characteristics

Typical local *Nu* is shown in Fig. 2(a) varying with Re_D at a specified heat flux. The curves with different line styles correspond to different Re_D for constant-property water, while the curves with markers refer to those for variable-property water. The curves depart from each other even for the constant-property cases as Re_D varying from 10 to 200. For higher Re_D, the *Nu* jumps to a higher value at the front of heated region, and then decays to $Nu_{CP,FD}$ within a longer distance downstream. The variable-property curves are always higher than their constant-property counterparts. Note that the variable-property curve for Re_D=10 is truncated at $X\approx12$ for inaccurate calculation, because after this location the fluid temperature is beyond 100 ℃ and thermophysical properties of liquid water are no longer available. The constant-property curve is not affected by this problem anyway, since the properties at T_0=20 ℃ are used in the computation.

Fig. 2(b) shows the distributions of the Δ*Nu*% along X for variable Re_D at a specified heat flux. It is clear that each curve indicates

an increase in the *Nu* enhancement and a drop downstream. Both the peak location and the slope of the curve vary with Re_D, which may lead to a seemingly valid conclusion that $\Delta Nu\%$ is a function of X and Re_D, for a specified heat flux and working liquid. It is described as 'seemingly', because the curves in Fig. 2(b) are quite similar with each other, with almost same peak value and same trend. Inspired by the classical reduction method of entrance problem (Shah and London, 1978), the dimensionless abscissa $X^+=X/Re_D=x/(DRe_D)$ is introduced, and the *Nu* and $\Delta Nu\%$ curves were expressed as its functions, as shown in Fig. 3.

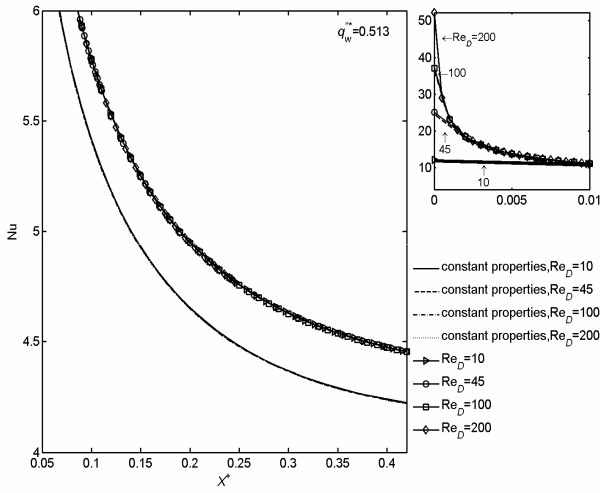

(a) Local *Nu* vs X^+

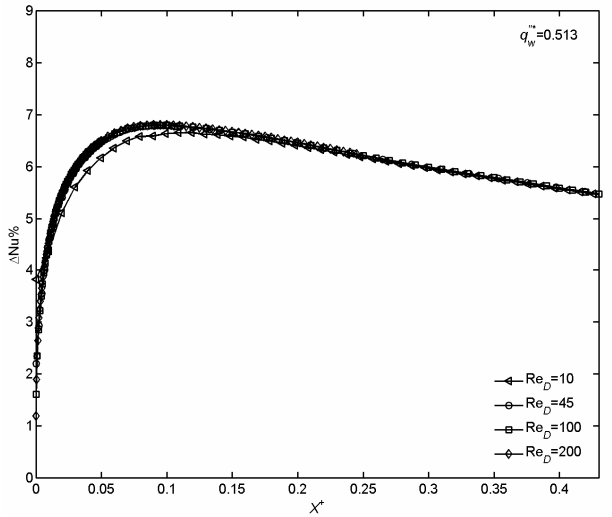

(b) Local $\Delta Nu\%$ vs X^+

Fig. 3. Entrance effect on heat transfer

As expected, the constant-property curves coincide with each other in most part of the heated region, except for the short starting area (See the small image in the upper-left of Fig. 3a). The small length of a departure near the starting point of heated region is mainly due to the axial fluid heat conduction, whose significance increases with a decreasing Re_D. The variable-property data, on the other hand, overlap to form another curve, which departs from the constant-property curve at a distance varying with X^+. The $\Delta Nu\%$ distributions show this phenomenon more directly that a single curve is formed, indicating the same heat transfer enhancement along X^+ at a specified heat flux. It turns out that $\Delta Nu\%$ is not the functions of X and Re_D separately, but their quotient. This implies that, on the functionary aspect, the variable-property mechanism performs as an amplifier of thermal development. The variable-property flow behavior, however, is quite different from constant-property developing flow, as elaborated in the following section.

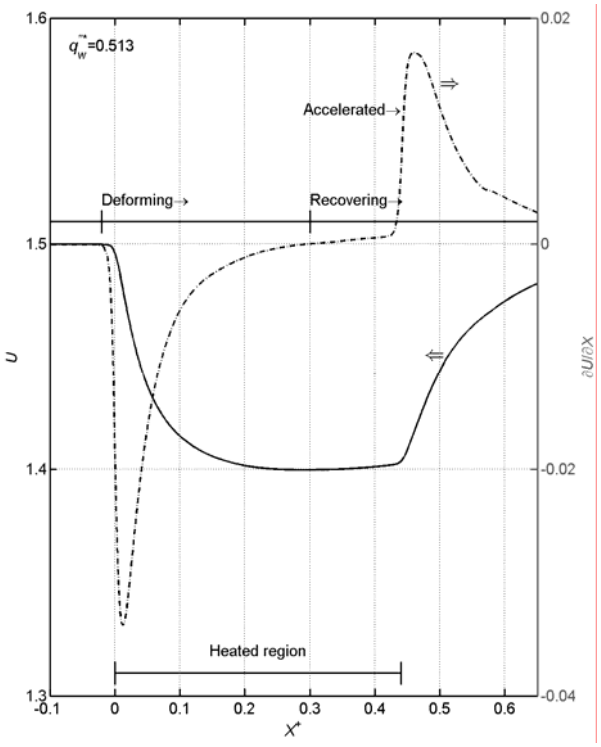

Fig. 4. Evolution of main-flow

3.2 Contributions of variable properties

The streamwise development of main-flow velocity, *U*, and its gradient is drawn at the centerline of the channel (symmetric plane) in Fig. 4. Since the fully-developed flow condition is given at the domain inlet, the

centerline velocity keeps the value of 1.5 for $X^+<0^-$. When the flow enters the heated region, due to high heat flux, dramatic spatial μ-variation takes place and distorts the parabolic *U*-*Z* profile, as shown in Fig. 5. The distorted profile varies together with temperature profile as the fluid heated along the flow until it achieves a most flattened profile. Afterward the flow undergoes a slow recovering process towards the parabolic profile until it leaves the heated region and accelerates to achieve fully developed flow at the absence of heating.

The cross-flow velocity component, *W*, is induced during the *U* variation process, out of necessity to satisfy the local mass conservation (Eq. (5)). Since this mechanism is originated from heat input, it is reasonable to infer that at a higher $q_w^{"*}$, a larger *W* is induced at a given streamwise location, which is proved in Fig. 6. The sign of *W* is always positive in the *U*-deforming part of heated region, since the flattened *U* profile forces an outward cross-section flow to the channel wall, which forms transverse convection as an enhancement to the heat removal from the wall. Though the entire scope of *W* is a small faction of *U*, the transverse convection is not negligible, contrary to popular belief, since the *W* is weighted by the cross-flow temperature gradient in the term of transverse convection, $W(\partial\theta/\partial Z)$ in Eq. (8). Hereby, the ratio of mean transverse to axial convection is defined as,

$$R_{conv} = \left(\int_0^{0.5} W \frac{\partial \theta}{\partial Z} dZ \right) \Bigg/ \left(\int_0^{0.5} U \frac{\partial \theta}{\partial X} dZ \right) \quad (18)$$

R_{conv} is calculated and presented in Fig. 7 for different heat fluxes. Obviously, for a typical case ($q_w^{"*} = 0.513$), a peak value of 4.3% is achieved at the vicinity of heated region front. The value of R_{conv} declines downstream to be zero at the position of largest *U* deformation, and then keeps going down to be minus (due to minus value of *W*, inward flow away from the channel wall) near the end of heated region. At a higher $q_w^{"*}$, R_{conv} increases to a higher peak value, and decreases more dramatically along the flow. At a small $q_w^{"*}$, in contrast, R_{conv} keeps to be a small positive value until the very downstream part of heated region.

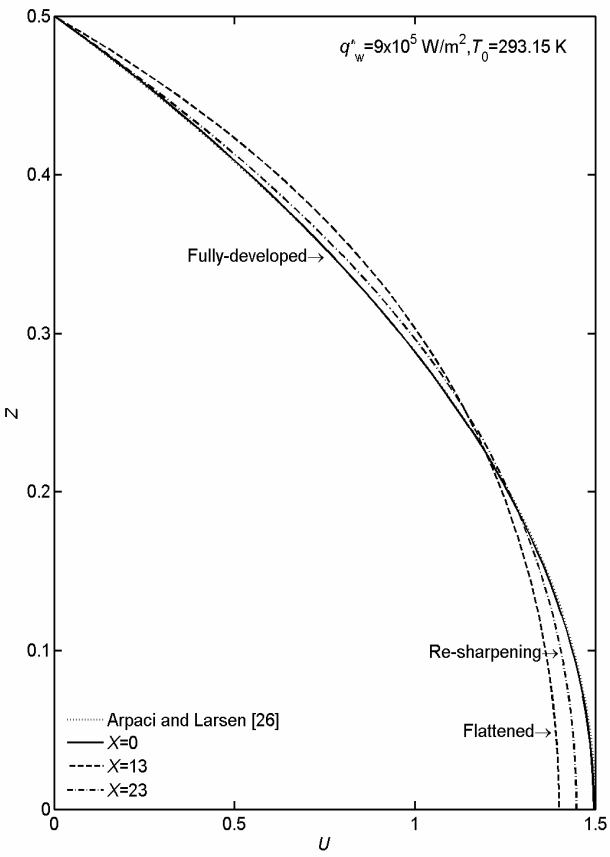

Fig. 5. Velocity profile evolution of main flow along flow direction

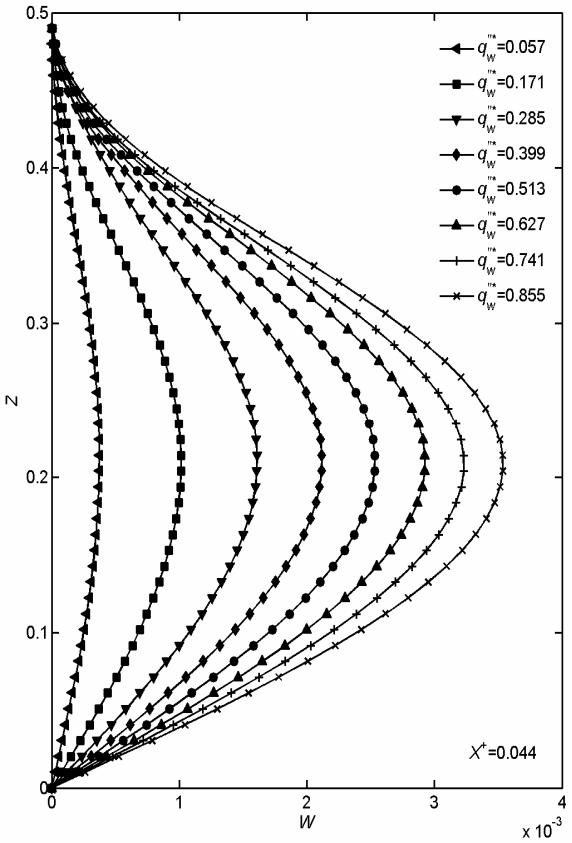

Fig. 6. Effect of heat flux on *W*-profile

Figs. 8 and 9 depict the *Nu* and Δ*Nu*% distributions, respectively, at different dimensionless wall heat fluxes, through which the effect of temperature-dependent viscosity is pronounced. It is found that the maximum Δ*Nu*% obtained is as large as 10% over the constant-property *Nu*, which should not be neglected. This can be made plausible by noting that the axial convection attributes to the enhancement of heat transfer, due to enlarged *U*-*Z* gradient for distorted *U* profile. It is worth noting that all the flow characteristics discussed in this section are unique for variable-property cases, due to the coupling mechanism from temperature field through μ-variation.

Even the temperature distribution itself, however, is not the same with constant-property thermal development, because of temperature-dependent thermal conductivity *k*. High temperature near the wall indicates higher *k*, which reversely promotes the heat removal from the wall and alters thermal diffusion. The *k*-variation along flow is also expected to affect the axial fluid conduction through the term in Eq. (8), or

$$\frac{1}{\mathrm{Re}_D \,\mathrm{Pr}}\left\{k^* \frac{\partial^2 \theta}{\partial Z^2} + \frac{\mathrm{Br}_{Sk}}{\mathrm{Br}_{qw}} S_k^* \left(\frac{\partial \theta}{\partial Z}\right)^2\right\} \qquad (19)$$

derived from $\dfrac{\partial}{\partial z}\left(k\dfrac{\partial T}{\partial z}\right) = k\dfrac{\partial^2 T}{\partial z^2} + \dfrac{\partial k}{\partial z}\dfrac{\partial T}{\partial z}$

in the dimensional energy equation. In the work of Mahulikar and Herwig (2006), the discussions on the role of *k*-variation were mostly on the scene of constant heat flux wall condition, for which the temperature profile along flow is almost linear, implying negligible second derivative of temperature. The axial conduction is then determined by the product $(\partial k/\partial z)\cdot(\partial T/\partial z)$. Comparison between the effects of "μ- and *k*-variations", "μ-variation only" and "*k*-variation only" were performed, showing "direct" and more significant enhancement of *Nu* for *k*-variation than μ-variation. It is a common understanding that the significance of fluid axial conduction effect is described using Peclet number, the product of *Re* and *Pr*. The *Nu* data in the reference (Mahulikar and Herwig, 2006), however, did not come along with Reynolds number specified, which weakened the persuasion of previously mentioned conclusion.

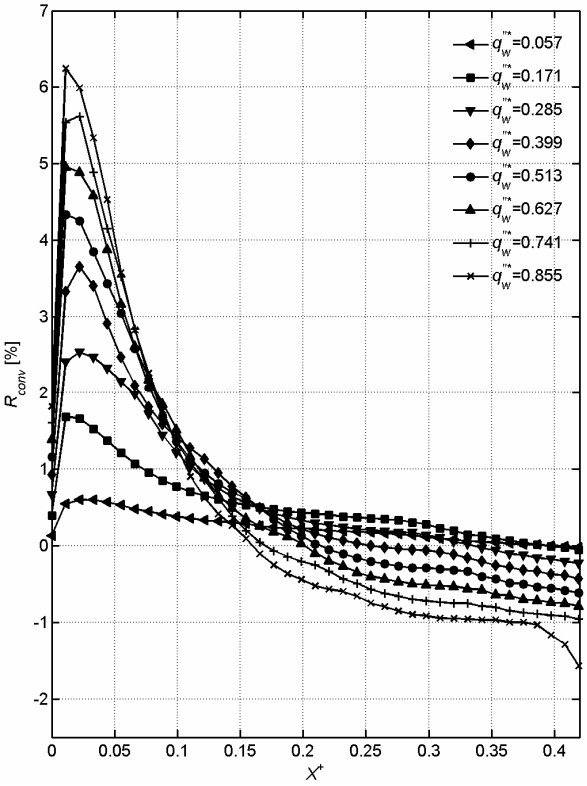

Fig. 7. Effect of heat flux $q_w^{"*}$ on R_{conv}

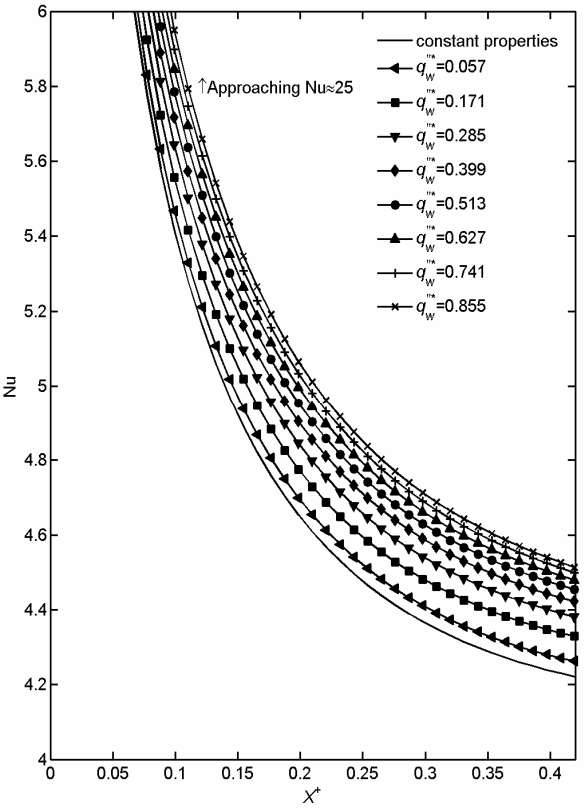

Fig. 8. Effect of heat flux $q_w^{"*}$ on local Nusselt number *Nu*

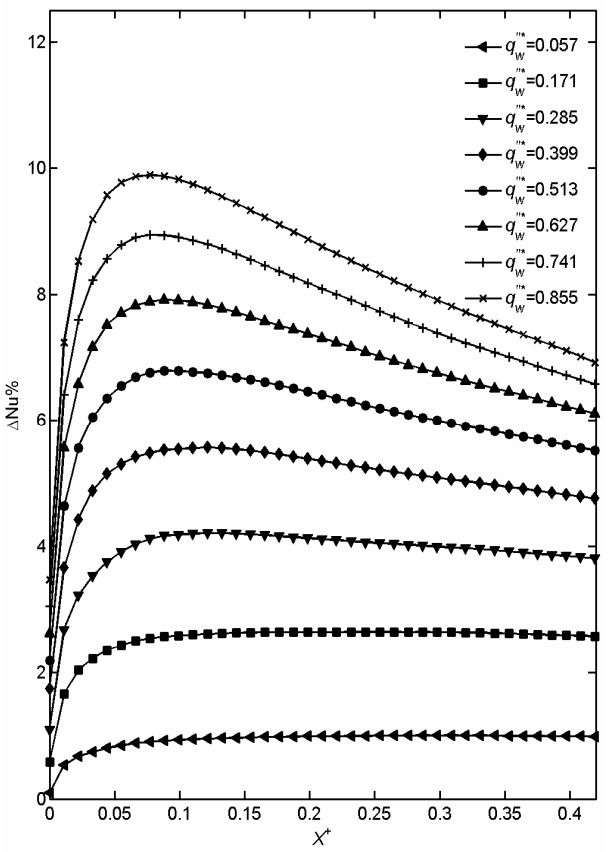

Fig. 9. Effect of heat flux q''^*_w on local Δ*Nu*%

The concerned heat transfer performance in present work, on the other hand, is evaluated at the presence of thermally developing flow. The second derivative of temperature in the axial conduction term is no longer negligible due to nonlinear variation of temperature profile along flow. Actually, the effect of fluid axial heat conduction on *Nu* for thermal entrance flow is not streamwisely uniform, as discussed in Shan and London (1978). They concluded that for *Pe*>10, the effect of fluid axial conduction was simply insignificant. The minimum *Pe* in present work is larger than 50 (larger than 200 in most cases). Thus it is not surprising that no *k*-variation influence is detectable in most cases of present work except for those at very low Reynolds numbers. (Note that the slight deviation of Re_D=10 curve from the others at the starting part of heated region, as shown in Fig. 3(b).)

4. Flow and Thermal Re-development

4.1 Velocity and temperature profiles

The streamwise development of main-flow velocity, *U*, and its gradient is drawn at the centerline of the channel (symmetric plane) in Fig. 4. The centerline velocity keeps the value of 1.5 for $X<0^-$, since the fully-developed flow condition is given at the domain inlet. When the flow enters the heated region ($X>0^+$), due to high heat flux, dramatic spatial μ-variation takes place and distorts the parabolic *U*-*Z* profile. Such developing process could be clearly seen in Fig. 5, showing *U*-*Z* profile at different streamwise locations. The distorted profile varies together with temperature increase as the fluid heated along the flow until it achieves a most flattened profile (approx. *X*=13).

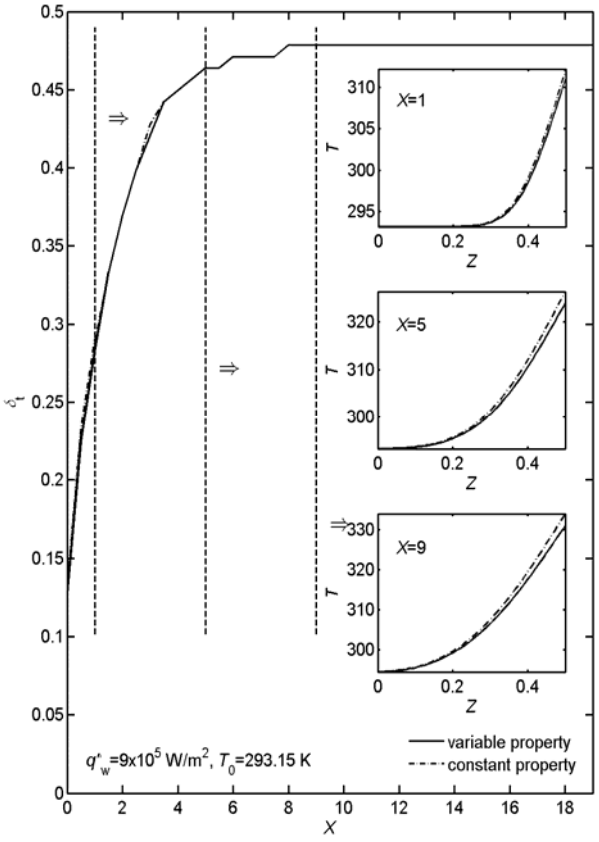

Fig. 10. Thermal development and cross-temperature profiles

Afterward the flow undergoes a slowly recovering process towards the parabolic profile until it leaves the heated region and accelerates to achieve fully developed flow at the absence of heating. This flow development is quite different, or rather opposite to that of normal entrance problems, since the velocity

profile develops outward to the channel wall and induces cross-flow velocity W to satisfy the local mass conservation. It is hereafter named 'flow re-development' in present work to distinguish the property-variation caused developing process from ordinary constant-property entrance problems. The re-developing flow enhances convection by introducing steeper velocity gradient adjacent to the wall. Additionally, transverse convection is also involved as an enhancement to the heat removal from the wall, in the term of $W(\partial\theta/\partial Z)$ in Eq. (8).

Regarding to the temperature distribution, it is generally believed that the thermal boundary layer thickness indicates the scale of temperature gradient across the flow and thus directly determines local heat transfer performance. Here the thermal boundary layer thickness, δ_t, is defined as the dimensionless distance from wall to the cross-sectional location where $(T_w\text{-}T)/(T_w\text{-}T_c)=0.999$. The developments of δ_t are depicted in Fig. 10 for variable- and constant-property flows, where the solid curve stands for variable-property flow and the dash-dot curve stands for constant-property flow. It is noticeable that the two curves very well overlap with each other, except slight departure in the beginning part of heated region. The cross-section temperature profiles are drawn at three typical streamwise locations, i.e., X=1, 5 and 9. At the vicinity of the front of heated region (X=1), variable-property temperature profile coincides with its constant-property counterpart along the flow section. As the fluid flows downwards, the two profiles begin to depart at the channel wall, but still merge into one curve near the centerline. For variable-property flow, the thermal conductivity is directly proportional to temperature for liquid water, thus $k_{w,VP}>k_0$ at high temperature near the wall. For constant-property flow, however, $k_{w,cp}=k_0$ at every location. Comparing the variable- with constant-property cases at a specified heat flux and x, the relation $\left(\partial T/\partial Z\right)_{w,VP} < \left(\partial T/\partial Z\right)_{w,CP}$ holds true since we have the relation of $q''_w = k_{w,VP}\left(\partial T/\partial Z\right)_{w,VP} = k_{w,CP}\left(\partial T/\partial Z\right)_{w,CP}$. Additionally, Fig. 10 also shows that $T_{w,VP}$ is always lower than $T_{w,CP}$. The wall temperature difference $\left(T_{w,CP} - T_{w,VP}\right)$ varies along the flow and exists even when thermal boundary layer thickness stops changing along the flow direction (approximately X>8).

Unlike the constant-property flow, there exist no "fully developed" flows for variable-property problem from either hydrodynamic or thermal point of view. This conclusion in the flow aspect is straight forward since the main-flow velocity keeps changing with varying viscosity along the heated region. Regarding to the thermal aspect, on the other hand, it is slightly confusable due to the converging thermal boundary development. Such confusion is actually caused by the definition of δ_t. As long as the thermal conductivity varies with increasing fluid temperature, the cross-section temperature profile changes unceasingly along the heated region and never achieves an unchanged "fully-developed" status. The concept of thermal boundary layer thickness, however, is unable to describe this variable-property phenomenon.

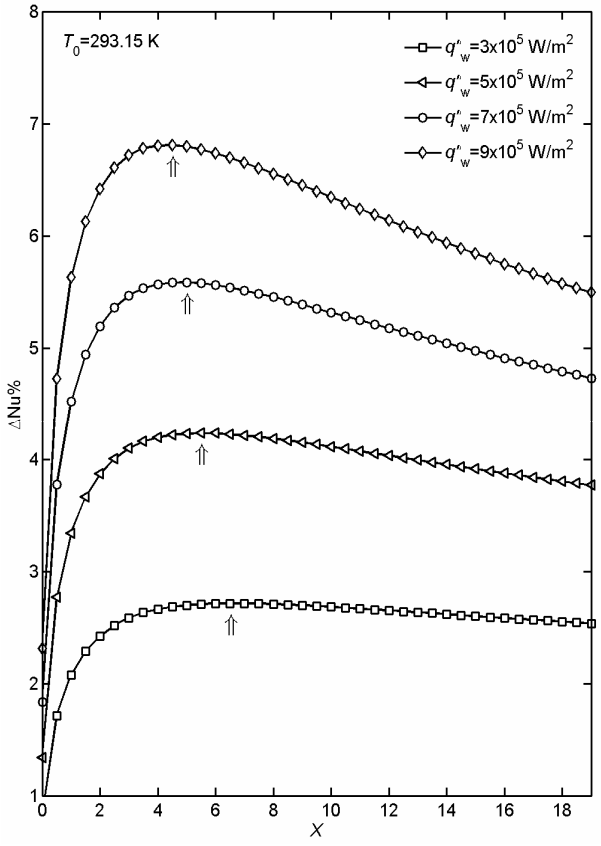

Fig. 11. Effect of heat flux on local $\Delta Nu\%$

4.2 Heat transfer enhancement behavior

Since the local heat transfer near the microchannel wall is the emphasized aspect in the present work, the local Nusselt number shall be an important parameter, as defined in Eq. (14).

It is intuitive to predict a steep *Nu* jump near the inlet of the heated region due to thin thermal boundary layer, regardless of variable- or constant-property flow, as hinted in Fig. 11. As the liquid flows downwards, the variable-property T_w begins to depart from the constant-property one. Since the bulk temperature, T_b, is defined in terms of the thermal energy transported by the fluid as it moves past the cross section, $T_{b,VP}$ keeps the same value with $T_{b,CP}$ at each streamwise location and a specified heat flux. Therefore, small $T_{w,VP}$ indicates higher heat transfer coefficient of variable-property flow than that of constant-property flow. The previous investigation (Liu et al., 2007, 2008) showed remarkable local Nusselt number increase in variable-property simulations, compared with constant-property results. This so-called variable-property effect was evaluated by the relative difference of local *Nu*, or defined in Eq. (16),

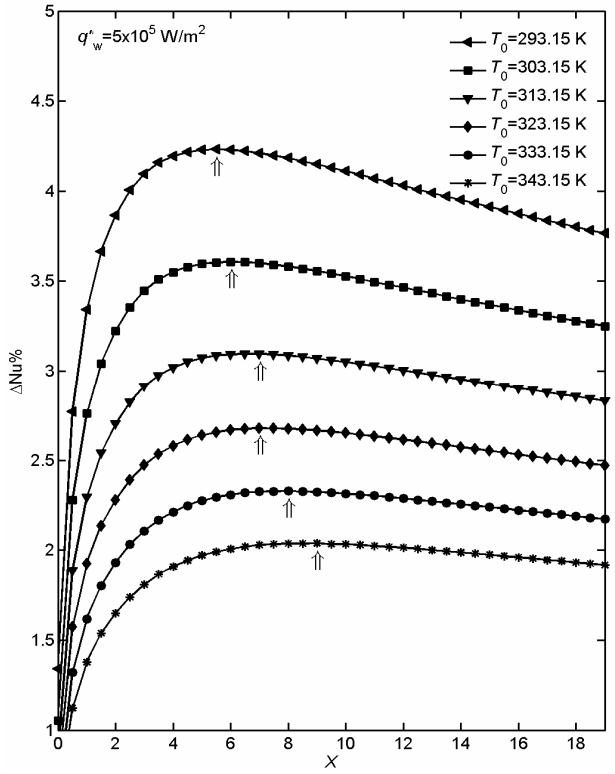

Fig. 12. Effect of inlet temperature T_0 on local $\Delta Nu\%$

Fig. 12 is a typical variable-property result showing the impact of heat flux on $\Delta Nu\%$ streamwise distributions at a specified inlet temperature. The $\Delta Nu\%$ curve starts from a low value at the immediate downstream of the inlet of the heated region, and climbs up dramatically along the *X*-axis. The peak value of $\Delta Nu\%$ appears at a distance of 4~10*D* from *X*-origin. Afterward, the curve declines gradually downwards. As concluded previously (Liu et al., 2007, 2008), the relative enhancement of the local Nusselt number due to the variable-property effect is a strong function of applied heat flux. A high heat flux results in a significant augment of $\Delta Nu\%$. Both the peak value and its location vary with the input heat flux as indicated by the up-arrows in Fig. 5.

The effect of inlet temperature is another concerned issue, which was rarely discussed in available investigations. As a similar phenomenon noted in Fig. 5, single-peaked $\Delta Nu\%$~*X* curves are also presented in Fig. 12 for different inlet temperatures at a specified heat flux. Both the intensity and effective coverage of enhanced heat transfer are affected by inlet temperature, lying in the fact that with increasing T_0, the peak value of $\Delta Nu\%$ curve declines, while the peak location moves downstream.

5. Analytical Description

5.1 Correlations

The above-conducted observations and discussions imply that both q''_w and T_0 are important parameters on the variable-property enhancement of *Nu*. In seeking a mathematical description on this issue, rather than observation merely based on figures, two parameters, $\Delta Nu\%_{max}$ and X_{max}, are introduced expressing the peak value and location of the $\Delta Nu\%$~*X* distribution, respectively.

The $\Delta Nu\%_{max}$ data calculated from simulation results are shown in Fig. 13. For a specified T_0, $\Delta Nu\%_{max}$ proportionally increases with increasing q''_w, whereas the impact of increasing T_0 results in declined $\Delta Nu\%_{max}$ at a specified heat flux. These two

trends, shown in Fig. 13(a), are in consistency with the observation in the simulations. Since q''_w and T_0 are the concerned factors in present problem with other conditions unchanged, it naturally implicates the relationship described using a function of $\Delta Nu\%_{max} = f\left(q''_w, T_0\right)$. For the convenience of discussion, the following form of function is boldly proposed, or

$$\Delta Nu\%_{max} = Cq''^{A}_{w} T_0^{B} \tag{20}$$

where A, B, and C are empirical constants independent of q''_w and T_0, and obtained as A=0.8528, B=-4.695, C=2.2158×10^7 from simulation results.

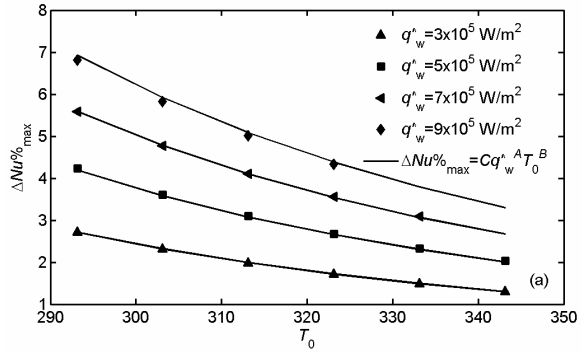

(a) Effect of heat flux

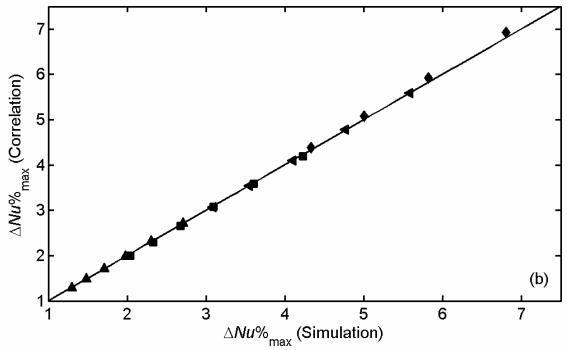

(b) Relative error

Fig. 13. Comparison of simulation with empirical correlation

Applying all conditions of q''_w and T_0 into Eq. (20) with the constants, predicted values of $\Delta Nu\%_{max}$ are compared with data from the numerical results at corresponding conditions, as shown in Fig. 13(b). A maximum absolute value of relative error is obtained as low as 1.68%, indicating that the power-law type function is compliant with the data characteristics, and that the processing procedure is under tight control of accuracy.

Fig. 14 shows the peak locations X_{max} of $\Delta Nu\%$~X curves. A processing procedure is carried out to X_{max} data based on the correlated function form as,

$$X_{max} = cq''^{a}_{w} T_0^{b} \tag{21}$$

The average constants are then obtained as a=-0.3380, b=2.796 and c=5.8345×10^{-5}. As shown in Fig. 14(b), the prediction by Eq. (21) agrees well with the simulation data within a maximum absolute value of relative error as low as 4.18%.

The effects of q''_w and T_0 on X_{max} are clearly shown in Fig. 14(a). For a small value of X_{max}, peak value of Nusselt number enhancement appears near the beginning of heated region, indicating large effective region of variable-property effect. From this point of view, a high heat flux not only results in increasing local heat transfer rate (high $\Delta Nu\%_{max}$ in Eq. (20)), but also achieves large coverage of the enhanced heat transfer (small X_{max} in Eq. (21)). Contrarily, a high inlet temperature shows quite negative impact on variable-property effect in terms of weakened intensity as well as limited effective coverage.

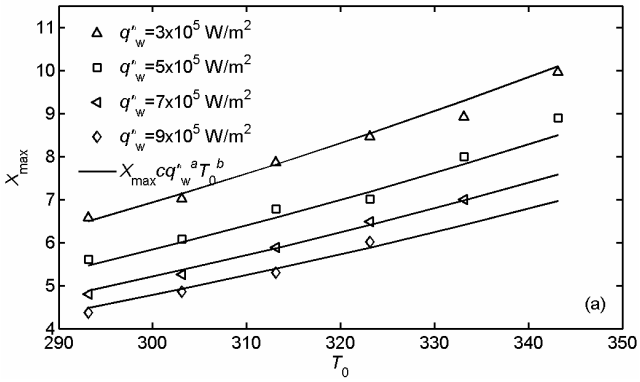

(a) Effect of heat flux

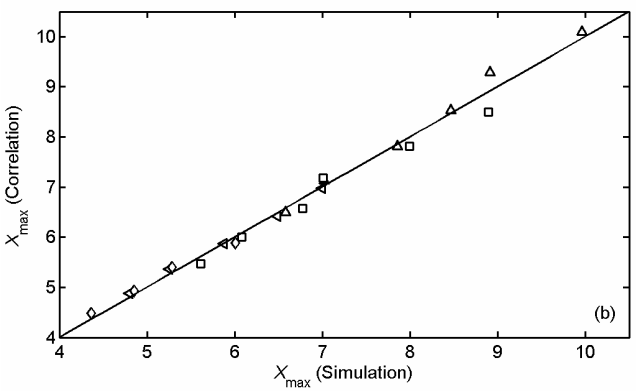

(b) Relative error

Fig. 14. Comparison of simulated X_{max} with empirical correlation

5.2 Theoretical approach

From the definition of Nu and $\Delta Nu\%$, or Eqs. (14) and (16), it is not difficult to derive the following expression,

$$\Delta Nu\% = \frac{k_0 \left(T_\mathrm{w} - T_\mathrm{b}\right)_\mathrm{CP}}{k_m \left(T_\mathrm{w} - T_\mathrm{b}\right)_\mathrm{VP}} - 1 \qquad (22)$$

Note that in constant-property flow both the thermal conductivity and (T_w-T_b) keep the same value at a specified heat flux and inlet temperature. In variable-property flow, on the other hand, k_m and (T_w-T_b) vary along the channel, resulting in the X-dependent $\Delta Nu\%$ behavior. The viscosity variation is also involved through the interaction of velocity and temperature fields, as discussed above.

As a successful attempt of theoretical approach, the Asymptotic Theory method provided the following form of Nu correction formula in variable-property problems as, (Liu et al., 2008)

$$\frac{Nu}{Nu_\mathrm{CP}} = 1 + \varepsilon \left[\begin{array}{l} K_k \bar{h}_B + K_\rho \left(\dfrac{206}{605} - \dfrac{232}{1815} \dfrac{1}{Pr_0} \right) \\ -K_\mu \dfrac{13}{121} + K_k \dfrac{148}{605} + K_c \dfrac{309}{1210} \end{array} \right] + 0\left(\varepsilon^2\right) \qquad (23)$$

where $\varepsilon = \dfrac{11}{24} \dfrac{q''_\mathrm{w} R}{k_0 T_0}$, $\bar{h}_B = \dfrac{48}{11 Pr_0} x$, and $K_\alpha = \left(\dfrac{T}{\alpha} \dfrac{\mathrm{d}\alpha}{\mathrm{d}T} \right)_0$ (α denotes ρ, k, μ or c_p).

The variation of thermal conductivity and viscosity of liquid water are considered. Following the definition of $\Delta Nu\%$, Eq. (23) is rearranged as,

$$\Delta Nu\% = \frac{11}{24} \frac{q''_\mathrm{w} R}{k_0 T_0} \left[K_k \frac{48}{11 Pr_0} x - K_\mu \frac{13}{121} + K_k \frac{148}{605} \right] + 0\left(\varepsilon^2\right) \qquad (24)$$

For a small heat transfer rate, both the second- and higher-order terms are neglected in AT method, which is also called *linear theory* by the authors (Herwig, 1985). Such simplification results in a linear relation of $\Delta Nu\%$~x, since all parameters remain unchanged for a specified q''_w and T_0 in Eq. (23). A straight forward inference of the linear theory is that the enhancement of Nu dependent upon the variable-property unceasingly amplifies along the flow as long as the fluid is heated. Such phenomenon is apparently not observed in above discussions, as shown in Sections 4.2 and 5.1. Alternatively, noticeable $\Delta Nu\%$~x peak is detected in each investigated case. It is therefore concluded that for large heat flux conditions (in the range of greater than 10^5 W/m^2), higher-order variable-property deviations over constant property are significant and should be theoretically modeled.

6. Conclusions

Numerical investigations were conducted in an effort to perform an in-depth analysis for microchannel convections, particularly to verify the variable-property effect of thermally developing flow in microchannels. Localized non-successive high heat flux boundary condition is frequently encountered in practical applications of microchannel heat exchangers and/or cooling devices, which results in steep temperature rise and dramatic property variation of working liquids in both flow and cross-flow directions. By considering liquid water of μ– and k-variation with temperature, two-dimensional convection in a D=100 μm single channel was theoretically modeled and numerically solved for different heat fluxes and Reynolds numbers. The following conclusions could be drawn from the results.

1. The velocity field is highly coupled with temperature distribution and distorted through the variation of μ and k. The induced cross-flow velocity W has non-negligible contribution to the convection. The heat transfer enhancement due to the μ-variation in the thermal developing process is pronounced, while the effect of k -variation on heat transfer is relatively insignificant.
2. Both flow and thermal re-development were observed due to the temperature-dependent viscosity and thermal conductivity. Such re-development resulted in marked heat transfer enhancement near the channel wall. The

local enhancement behavior was described by defining the peak value and location of relative Nusselt number distribution as $\Delta Nu\%_{max}$ and X_{max}, which reflected the variable-property effect intensity and effective region, respectively. The impacts of heat flux and inlet temperature were discussed. To verify the contributing factors, power-law functions were assumed in the data reduction process at the convenience of discussion, which provided reasonable trend and good accuracy.

3. The single-peaked $\Delta Nu\%$~X variation in present work disagrees with the linear relation suggested by the Asymptotic Theory method, since the large heat flux and dramatic temperature rise induces higher-order terms of property variation, which was not included in the linear scope of AT method. Apparently, the strong nonlinear mechanism prevailed in the present relation of $\Delta Nu\%_{max}$ and X_{max}. Both peak value and location are introduced to understand such kind of problems, which should be quite important in both industrial designing and scientific researches.

Acknowledgement

This investigation is currently supported by the National Natural Science Foundation of China (Grant No. 50636030).

References

Adams, T.M., Abdel-Khalik, S.I., Jeter, S.M., Qureshi, Z.H., 1998. An experimental investigation of single-phase forced convection in microchannels. International Journal of Heat and Mass Transfer 41 (6-7), 851-857.

Arpaci,V.S., Larsen, P.S., 1984. Convection heat transfer, Prentice-Hall, London.

Bird, R.B., Stewart, W.E., Lightfoot, E.N., 2002. Transport Phenomena, 2nd ed.. John Wiley & Sons, New York.

Del Giudice S., Nonino, C., Savino, S., 2007. Effects of viscous dissipation and temperature dependent viscosity in thermally and simultaneously developing laminar flows in microchannels. Int. J. Heat Fluid Flow 28, 15-27.

Fedorov, A.G., Viskanta, R., 2000. Three-dimensional conjugate heat transfer in the microchannel heat sink for electronic packaging. International Journal of Heat and Mass Transfer 43 (3), 399-415.

Gamrat, G., Marinet, M.F., Asendrych, D., 2005. Conduction and entrance effects on laminar liquid flow and heat transfer in rectangular microchannels. International Journal of Heat and Mass Transfer 48 (14), 2943-2954.

Graetz, L., 1883. Under die Warmeleitungsfahigkeit von Flussigkeiten (On the thermal conductivity of fluids) Part1. Ann. Phys. Chem. 18, 79-94.

Harms, T.M., Kazmierczak, M., Gerner, F.M., Holke, A., Henderson, H.T., Pilchowski, J., Baker, K., 1997. Experimental investigation of heat transfer and pressure drop through deep microchannels in a (110) silicon substrate. in: Proceedings of the 1997 ASME International Mechanical Engineering Congress and Exposition, ASME, Dallas, TX, USA, pp. 347-357.

Herwig, H., 1985. Effect of variable properties on momentum and heat transfer in a tube with constant heat flux across the wall. Int. J. Heat Mass Transfer 28, 423-431.

Herwig, H., Mahulikar, S.P., 2006. Variable property effects in single-phase incompressible flows through microchannels. Int. J. Therm. Sci. 45, 977-981.

Holman, J.P., 1997. Heat transfer. 8th ed, McGraw-Hill, London.

Kandlikar, S.G., Joshi, S., Tian, S., 2003. Effect of surface roughness on heat transfer and fluid flow characteristics at low Reynolds numbers in small diameter tubes. Heat Transfer Engineering 24 (3), 4-16.

Kumar, V., Gupta, P., Nigam, K.D.P., 2007. Fluid flow and heat transfer in curved tubes with temperature-

dependent properties. Ind. Eng. Chem. Res. 46, 3226-3236.

Liu, J.T., Peng, X.F., Wang, B.X., 2008. Variable-property effect on liquid flow and heat transfer in microchannels. Chemical Engineering Journal 141, 346-353.

Liu, J.T., Peng, X.F., Yan, W.M., 2007. Numerical study of fluid flow and heat transfer in microchannel cooling passages. Int. J. Heat Mass Transfer 50, 1855-1864.

Mahulikar, S.P., Herwig, H., 2005. Theoretical investigation of scaling effects from macro-to-microscale convection due to variations in incompressible fluid properties. Applied Physics Letters 86 (1), 014105.

Mahulikar, S.P., Herwig, H., 2006. Physical effects in laminar microconvection due to variations in incompressible fluid properties. Physics of Fluids 18 (7), 073601.

Ng, E.Y.K., Tan, S.T., 2004. Computation of three-dimensional developing pressure-driven liquid flow in a microchannel with EDL effect. Numerical Heat Transfer; Part A: Applications 45 (10), 1013-1027.

Nonino, C., Giudice, S.D., Savino, S., 2006. Temperature dependent viscosity effects on laminar forced convection in the entrance region of straight ducts. Int. J. Heat Mass Transfer 49, 4469-4481.

Nusselt, W., 1910. Die Abhangigkeit der Warmeu bergangszahl von der Rohrlange (The relation between heat transmission and length of pipe). Z. Ver. Deutscher Ing.

Palm, B., 2001. Heat transfer in microchannels. Microscale Thermophysical Engineering 5 (3), 155-175.

Pantokratoras, A., 2007. Fully developed forced convection of three fluids with variable thermophysical properties flowing through a porous medium channel heated asymmetrically with large temperature differences. J. Porous Media 10, 409-419.

Peng, X.F., Peterson, G.P., 1996. Forced convection heat transfer of single-phase binary mixtures through microchannels. Experimental Thermal and Fluid Science 12 (1), 98-104.

Peng, X.F., Wang, B.X., 1993. Forced convection and flow boiling heat transfer for liquid flowing through microchannels. International Journal of Heat and Mass Transfer 36 (14), 3421-3427.

Pfahler, J., Harley, J., Bau, H., Zemel, J., 1990. Liquid transport in micron and submicron channels. Sensors and Actuators 22 (1-3), 431-434.

Qu, W., Mudawar, I., 2002. Analysis of three-dimensional heat transfer in micro-channel heat sinks. International Journal of Heat and Mass Transfer 45 (19), 3973-3985.

Qu, W., Mudawar, I., Lee, S.Y., Wereley, S.T., 2006. Experimental and computational investigation of flow development and pressure drop in a rectangular micro-channel. Journal of Electronic Packaging, Transactions of the ASME 128 (1), 1-9.

Rahman, M.M., Gui, F., 1993. Experimental measurements of fluid flow and heat transfer in microchannel cooling passages in a chip substrate. in: Proceedings of the ASME International Electronics Packaging Conference, ASME, Binghamton, NY, USA, pp. 685-692.

Seddeek, M.A., Salem, A.M., 2006. Further results on the variable viscosity with magnetic field on flow and heat transfer to a continuous moving flat plate. Phys. Lett. A 353, 337-340.

Shah, R.K., London, A.L., 1978. Laminar flow forced convection in ducts: A Source Book for Compact Heat Exchanger Analytical Data. Academic Press, New York.

Sherman, F.S., 1990. Viscous Flow, McGraw-Hill, New York.

Sieder, E.N., Tate, C.E., 1936. Heat transfer and pressure drop of liquids in tubes. Industrial Engineering Chemistry 28, 1429.

Sobhan, C.B., Garimella, S.V., 2001. A comparative

analysis of studies on heat transfer and fluid flow in microchannels. Microscale Thermophysical Engineering 5 (4), 293-311.

Tan, S.T., Ng, E.Y.K., 2006. Numerical analysis of EDL effect on heat transfer characteristic of 3-D developing flow in a microchannel. Numerical Heat Transfer; Part A: Applications 49 (10), 991-1007.

Tuckerman, D.B., Pease, R.F.W., 1981. High-performance heat sinking for VLSI. IEEE Electron Device Letters ED-2 (5), 126-129.

Wagner, W., Berlin, A.K., 1998. Properties of water and steam: the industrial standard IAPWS-IF97 for the thermodynamic properties and supplementary equations for other properties. Springer-Verlag, New York.

Wang, B.X., Peng, X.F., 1994. Experimental investigation on liquid forced-convection heat transfer through microchannels. International Journal of Heat and Mass Transfer 37 (suppl. 1), 73-82.

Wu, P., Little, W.A., 1983. Measurement of friction factors for the flow of gases in very fine channels used for microminiature Joule-Thomson refrigerators. Cryogenics 23 (5), 273-277.

Wu, P., Little, W.A., 1984. Measurement of the heat transfer characteristics of gas flow in fine channel heat exchangers used for microminiature refrigerators. Cryogenics 24 (8), 415-420.

Yang, C., Li, D., Masliyah, J.H., 1998. Modeling forced liquid convection in rectangular microchannels with electrokinetic effects, International Journal of Heat and Mass Transfer 41 (24), 4229-4249.